Minimal Order Compensator Design for a DC-to-DC Power Converter

Sam Jacobs, Richard Tymerski
Maseeh College of Engineering and Computer Science
Portland State University
Portland, Oregon

***Abstract*—In this paper we undertake the designs of two reduced order compensators for a (fourth order) switching dc-to-dc converter. For each, the design methodology of modern control theory is utilized in that optimal controller gains are derived using the linear quadratic regulator (LQR) methodology and state estimators with loop transfer recovery (LTR) are designed to obviate the need for state measurement and to ensure desirable loop gain characteristics. The resulting compensators, in each case, are further order reduced whereby states with relatively small Hankel singular values are discarded. In the first case, the final third order compensator design is achieved by model reducing the fifth order transfer function of a loop transfer recovered (four state) full order estimator together with (one state) integral control. In the alternative design, model reduction is applied to the transfer function of a loop transfer recovered (three state) reduced order estimator together with (one state) integral control, resulting in a second order compensator. In terms of implementation, the second design approach is seen as more favorable. A practical implementation is shown and simulated verifying the design efficacy.**

***Index Terms*—linear quadratic regulator (LQR), estimator, loop transfer recovery (LTR), model order reduction, dc-to-dc converter**

I. Introduction

The design of compensators or controllers for dc-to-dc power converters may be undertaken from a classical control or modern control perspective [1], [9]. The mathematical system description used in a classical control framework is the transfer function. Whereas modern control uses the time domain description of state equations. The predominant classical control design paradigm is that of loop shaping; whereas under modern control it is pole placement. Under a full state feedback control law, and for a fully controllable system, poles may be placed in any desired locations in the s-plane. Prevalent under the modern control framework is the use of optimization formulations whereby pole locations are not decided directly but rather a cost function is minimized. One such example is the linear quadratic regulator (LQR) formulation where a quadratic cost function involving the system state and inputs is minimized. This formulation inherently results in the ability to penalize state and/or input variations. Further advantages of optimal control are guaranteed performance specifications such as stability margins under LQR control. Thus we see that modern control designs have advantages over traditional classical control methods.

In this paper, we use the modern control framework to design controllers for the C1 dc-to-dc converter which is discussed in the next section. Specifically, an LQR design is undertaken and then followed up by full order and reduced order estimator designs, which obviates the need for state measurements. However, both these estimator designs need to be undertaken using a loop transfer recovery (LTR) approach in order to recover the desirable loop properties of the LQR design. Finally, the important issue of compensator implementation needs to be addressed. This then directs attention to the order of the compensator transfer function and in particular its minimization while maintaining good performance. This is subsequently achieved using a method which removes the states with the lowest energy contribution to overall model behavior.

An outline for the paper is as follows. In the next section the C1 dc-to-dc converter is introduced and a state space model is developed. In Section III an LQR design is given. A full order estimator (FOE) design using LTR, referred to as FOE/LTR, is undertaken in Section IV. The subsequent compensator comprising the LQR control law and the FOE/LTR is next order reduced in Section V to obtain the minimal order compensator transfer function. Sections VI and VII, tackle the case of the reduced order estimator, i.e. ROE/LTR, and the final compensator transfer function, as one might expect, is found to be of lower order than that obtained from the FOE/LTR design. Implementation of the reduced ROE/LTR compensator is presented in Section VIII and simulation results are given which verify the design.

II. The C1 DC-to-DC Converter

The power processing system used in our study is the dc-to-dc switching power converter shown in Figure 1. This converter is one of many that was derived in [2] and [3] and is named the C1 converter due to its position in a classification matrix of converters. Further discussion of this converter has been provided in [4] and [5]. In our study the converter will be used to regulate a 10 volt DC input down to 5 volts across a load represented by resistor R, which has a value of 5 ohms. The values of the inductors and capacitors are as follows:

$L_1 = 300\mu F$, $L_2 = 680\mu F$, $C_1 = 10\mu F$ and $C_2 = 10\mu F$. The converter operates at a nominal switching frequency of 100 kHz. As a performance measure we will examine the effect of input voltage disturbances on the output voltage. A 10% step (i.e. 1 V) in the input voltage will be used. Figure 2 shows the open loop response of the system as obtained using the PECS simulation software [6], [7]. Clearly seen is the high degree of ringing and the dc output voltage offset from the desired 5 volts that the closed loop system is tasked to eliminate.

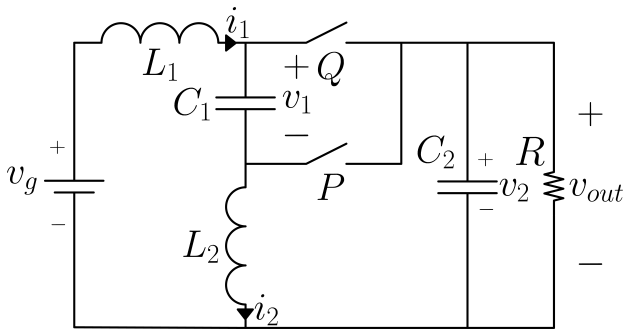

Fig. 1. The C1 dc-to-dc converter

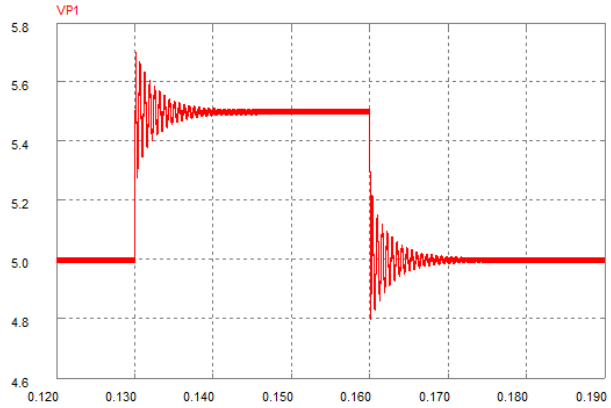

Fig. 2. Output of the C1 converter due to a unit step changes of input voltage from 10 volts to 11 volts back top 10 volts.

Modern control design methodology requires a minimal state space representation of the converter. This is obtained using the state space averaging method [8], [9] to yield a small signal model. Since the system switches between two switched states, we model each switched state individually then create a model based upon the weighted averages of the two states. The state space model for the converter is then be represented by the small signal average:

$$\dot{x} = Ax + Bv_g + B_d d$$

$$y = Cx + Ev_g + E_d d$$

where x, v_g, d and y represent the state, input voltage, duty ratio and output voltage, respectively. The state is given by the inductor currents and capacitor voltages, i.e. $x = [v_2,\ v_1,\ i_2,\ i_1]^T$.

Each switched state is represented with the standard space model equations. For the first switched state where the switches, Q and P, shown in Figure 1, are in their ON and OFF states, respectively, the state matrices are:

$$A_1 = \begin{bmatrix} \frac{-1}{RC_2} & 0 & \frac{-1}{C_2} & \frac{1}{C_2} \\ 0 & 0 & \frac{1}{C_1} & 0 \\ \frac{1}{L_2} & \frac{-1}{L_2} & 0 & 0 \\ \frac{-1}{L_1} & 0 & 0 & 0 \end{bmatrix}$$

$$B_1 = \begin{bmatrix} 0 & 0 & 0 & \frac{1}{L_1} \end{bmatrix}^T$$

$$C_1 = \begin{bmatrix} 1 & 0 & 0 & 0 \end{bmatrix}$$

$$E_1 = 0$$

For the second switched state, where switches Q and P are now in their OFF and ON states, respectively, the state matrices are:

$$A_2 = \begin{bmatrix} \frac{-1}{RC_2} & 0 & \frac{-1}{C_2} & \frac{1}{C_2} \\ 0 & 0 & 0 & \frac{1}{C_1} \\ \frac{1}{L_2} & 0 & 0 & 0 \\ \frac{-1}{L_1} & \frac{-1}{L_1} & 0 & 0 \end{bmatrix}$$

$$B_2 = \begin{bmatrix} 0 & 0 & 0 & \frac{1}{L_1} \end{bmatrix}^T$$

$$C_2 = \begin{bmatrix} 1 & 0 & 0 & 0 \end{bmatrix}$$

$$E_2 = 0$$

For the C1 converter the steady state average output/input DC voltage relationship is given by $\frac{V}{V_g} = D$, where D represents the steady state duty ratio. For our system we require an output voltage of 5 Volts with a nominal input of 10 Volts, therefore the steady state duty ratio is $D = 0.5$. With the known duty ratio, we can write a state space averaged model with the following relationships.

$$D' = 1 - D$$

$$A = DA_1 + D'A_2$$

$$B = DB_1 + D'B_2$$

$$C = DC_1 + D'C_2$$

$$E = DE_1 + D'E_2$$

Please note that we use E in this section to denote the feed-forward matrix. In other sections we will use the more standard name D when we do not need to distinguish it from the duty ratio term.

The steady state values for the state and input are denoted by X and V_g, respectively. These are used in the final set of matrices:

$$X = -A^{-1}BV_g$$

$$B_d = (A_1 - A_2)X + (B_1 - B_2)V_g$$

$$E_d = (C_1 - C_2)X + (E_1 - E_2)V_g$$

This completes the open loop model for the system.

III. Linear Quadratic Regulator

We wish to design a compensator that achieves precise regulation of the system output voltage while eliminating steady state error. The linear quadratic regulator (LQR) compensator is a full state feedback compensator. It will feedback a weighted sum of state values to the plant control input d, so that:

$$d = -k_a^T x_a$$

x_a is the augmented vector consisting of the plant's state variables and single new state, x_i, which is the output of an integrator added to the compensator in order to achieve zero steady state error to a step input. This integrator takes an input that is the difference between the desired output y_d and the actual output, y. Therefore:

$$x_a = \begin{bmatrix} x \\ x_i \end{bmatrix}$$

where

$$x_i = \int_0^t (y_d - y)\,\mathrm{d}\tau$$

and $k_a = [k \quad k_i]$ is a vector of gains which is chosen to move the poles of the overall system to desired locations. However, rather than directly deciding where to place poles, we supply cost penalty matrices Q and R used as part of the LQR formulation, as discussed next. R is a positive definite matrix that places relative penalty on fluctuation on the control input. Q is a positive semi-definite matrix that places relative penalty on fluctuation in the plant's states. Together, the Q and R matrices are used in minimizing the cost function:

$$J = \frac{1}{2}\int_0^\infty \left(x^T Q x + u^T R u\right)\,\mathrm{d}t$$

where u denotes the input, in general, which in our case is the duty ratio, d.

The Simulink diagram shown in Figure 3 implements the closed loop system where we have the ability to measure the plant state variables and feed them back via the k vector.

From our system matrices we see that $C_1 = C_2 = C$ and $E_1 = E_2 = 0$ which results in the output equation having the form

$$y = Cx$$

Together with the previous plant state equations and given that the desired output is constant, which implies that $y_d = 0$, results in the following small signal model of the system:

$$\dot{x}_a = \begin{bmatrix} A & 0 \\ -C & 0 \end{bmatrix} x_a + \begin{bmatrix} B \\ 0 \end{bmatrix} v_g + \begin{bmatrix} B_d \\ 0 \end{bmatrix} d$$

The design of the controller gains k_a is found by using the Matlab *lqr* function together with the matrices of this model and the Q and R penalty matrices, which are discussed next.

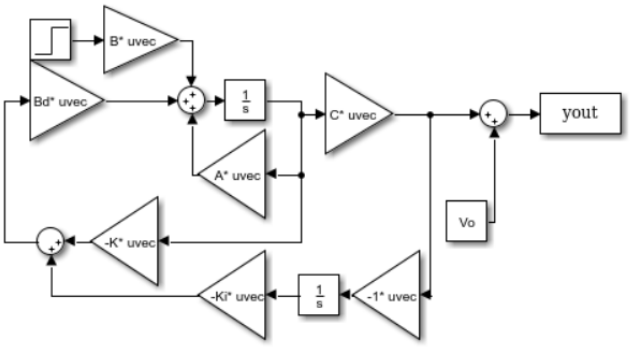

Fig. 3. LQR Compensator in Simulink.

Through trial and error we arrived at the following values for the penalty matrices:

$$Q = \begin{bmatrix} 1 & 0 & 0 & 0 & 0 \\ 0 & 0 & 0 & 0 & 0 \\ 0 & 0 & 0 & 0 & 0 \\ 0 & 0 & 0 & 0 & 0 \\ 0 & 0 & 0 & 0 & 100000 \end{bmatrix}$$

$$R = 1$$

This resulted in:

$$k_a = \begin{bmatrix} 0.5886 & -0.0162 - 1.6179 & 1.6141 & -316.2278 \end{bmatrix}$$

The above k_a values move the poles of the regulated system to -46142 ± 48931, $-863.59 \pm j9912$ and -315 in the s plane. As expected, all the poles are in the left side of the s plane, indicating a stable system. This k_a value was used in the Simulink model of Figure 3 and the response to a unit step disturbance input was obtained and is shown in Figure 4. Clearly the disturbance is greatly rejected by this closed loop system as seen by the output producing a maximum deviation of only 70 mV compared to the 700 mV deviation seen in Figure 2.

This completes the LQR portion of the controller design.

IV. Loop Transfer Recovery of Compensator with Full Order Estimator

As mentioned in the previous section, we do not wish to directly measure the state variables. Therefore we will use a full order esitmator with loop transfer recovery (LTR) derived compensator, hereafter referred to as a FOE/LTR compensator. The FOE/LTR compensator reuses the k_a values found in the previous section but derives an estimate of the state variables. The estimator is described by the following state equation:

$$\dot{\hat{x}} = A\hat{x} + B_d d + L(y - C\hat{x})$$

where $\hat{x}$ is the estimate of state variables x, and as before, d is the control input defined as $-k_a\hat{x}_a$ and y is the plant output. The estimator gain vector L is chosen to move the poles of the estimator to the desired location. (Note that, as

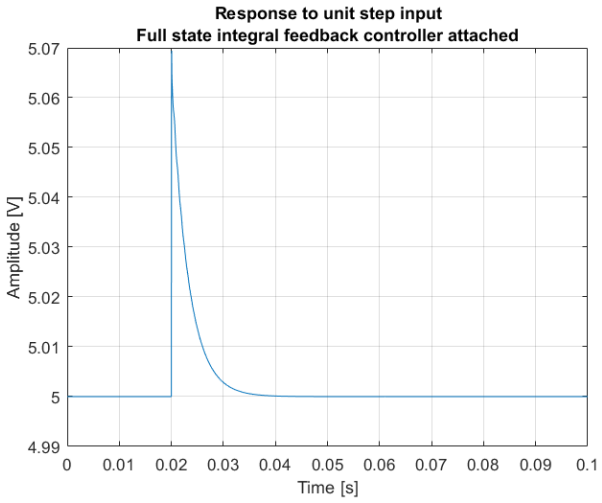

Fig. 4. LQR compensator response to unit step input.

a matter of convenience, the disturbance input is not fed into the estimator. The consequence of this is discussed later).

By using a compensator with an integrator full order estimator, we can describe the system in state space as:

$$\dot{x} = Ax - B_d k\hat{x} - B_d k_i x_i + Bv_g$$

$$\dot{x}_i = -Cx$$

$$\dot{\hat{x}} = LCx - B_d k_i x_i + (A - B_d k - LC)\hat{x}$$

$$y = Cx$$

The LQR procedure can be used to design for an optimal value of L resulting in the optimal estimator, which is also known as the Kalman filter. The resulting combination of optimal estimator with the optimal regulator is known as a Linear Quadratic Gaussian (LQG) design. Unfortunately, the combination of the two is not generally optimal. The LQG compensator does not have guaranteed stability margins [10], unlike the case for LQR design which uses state measurements. To overcome these lmlitations the Loop Transfer Recovery (LTR) design methodology was proposed [11], which seeks to replicate the optimal characteristics of an LQR compensator with full state feedback. Loop transfer recovery is an iterative procedure where we increase the weights in the cost function. We use the weights:

$$R = 1$$

$$Q = q^2 B_d B_d^T$$

and increase the value of scalar q until we have adequately recovered the loop transfer function of the full state feedback LQR compensator.

For the various Q and R values, we use the Matlab function *lqe*. Similiar to the function *lqr*, *lqe* finds the vector L as defined by:

$$L = \Sigma C^T R^{-1}$$

where Σ is the solution to the Algebraic Ricatti Equation (ARE):

$$0 = A\Sigma + \Sigma A^T + Q - \Sigma C^T R^{-1} C\Sigma$$

The loop we are recovering is the loop formed by disconnecting the controller output from the input of the plant. For this approach, we compared a few different values of q. Larger q values produce results closer to the LQR results. This can be seen in the Bode diagram in Figure 5 for the various values of q chosen.

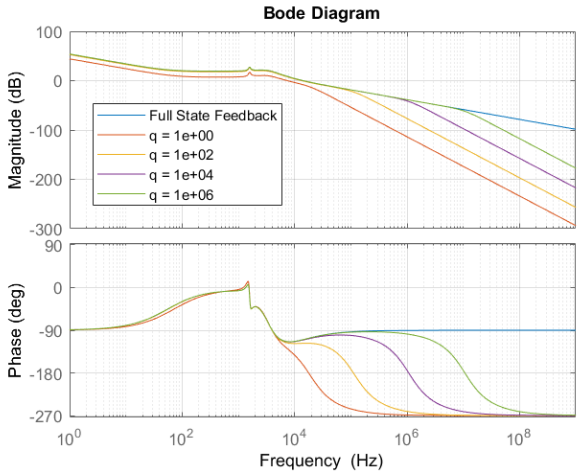

Fig. 5. Bode diagram of open loop system with full order estimator undergoing LTR.

q	Phase Margin	Bandwidth
Full State Feedback	70	14320
1	51	7427
100	62	13269
10000	69	14212
1000000	70	14309

TABLE I
STABILITY MARGINS FOR FOE/LTR SYSTEM AT VARIOUS q VALUES

Table I lists the phase margin (in degrees) and unity gain crossover frequency (in Hertz) of the FOE/LTR system as q increases. It can be seen that greater values of q come closer to recovering the stability margins of the original full state feedback LQR system. However, even lower q values yield viable stability margins. For our design, we settled on $q = 10^6$ which produced an L of:

$$L = \begin{bmatrix} 9.49 \cdot 10^7 & -1.00 \cdot 10^{11} & -1.47 \cdot 10^{10} & 3.03 \cdot 10^{10} \end{bmatrix}$$

which places estimator poles at $-4.7439 \cdot 10^7 \pm j4.7439 \cdot 10^7$ and $-866.34 \pm j9912.6$.

To examine the efficacy of this design we implemented the Simulink model shown in Figure 6. The Simulink model includes the plant model, the integral regulator (whose gains were derived in the prior LQR section), a full order estimator and an external disturbance input. Using the L just derived the output resulting by applying a unit step disturbance input is

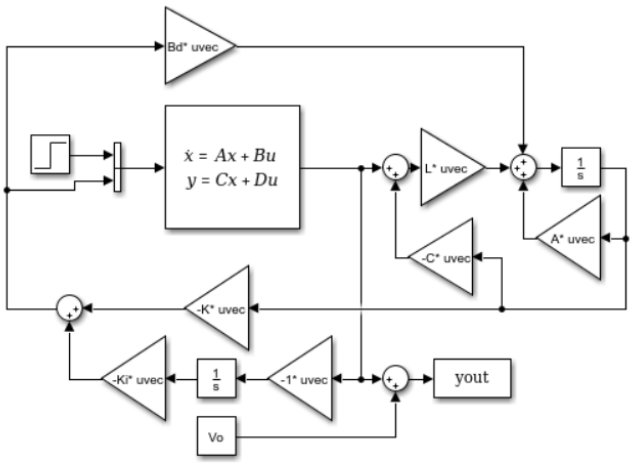

Fig. 6. Compensator with full order estimator in Simulink.

shown in Figure 7. Also shown for comparison in this figure is the response of the LQR design with measured states of the previous section. Clearly seen is the very close agreement between the two responses. Note, for simplicity, in Figure 6 the disturbance input is not fed into the estimator. Nevertheless the performance is good. More will be said about this later.

For a controller to be viable in this system, the duty ratio needs to be within the following limits $0 < D + d < 1$. Therefore, as further examination of the response of the system given the step input disturbance, we also looked at the control effort required, that is, the change in the control input that is needed to effect control. This is shown in Figure 8 for both the FOE/LTR and the previous section LQR with measured states design. Again we see very close agreement between the two responses and also verify that the duty ratio limits are not violated.

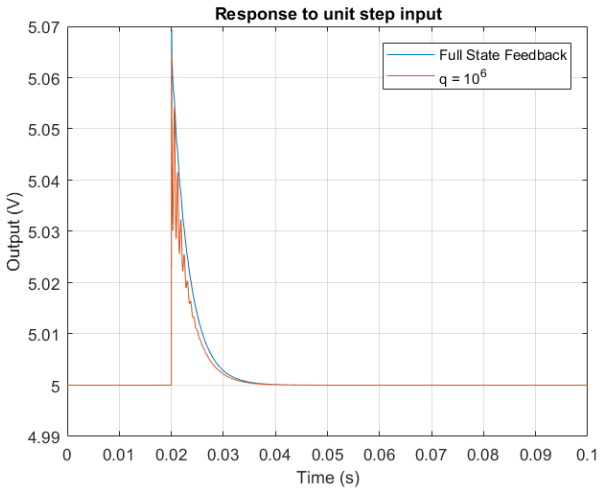

Fig. 7. Simulink results of response to unit step input for FOE/LTR system. Also shown is the response for the LQR with measured state design.

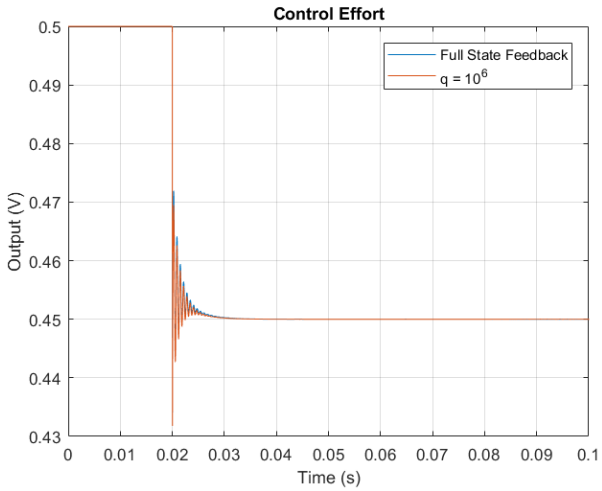

Fig. 8. Simulink results of control effort in response to unit step input for FOE/LTR system. Also shown is the response for the LQR with measured state design.

V. Model Reduction

The FOE/LTR compensator consists of an integrator and an estimator that replicates all four states of the plant. Therefore the compensator is fifth order. To simplify practical implementation we next consider reducing the order of the compensator.

To achieve model reduction, we chose to use the *balred* function in Matlab. Given our original transfer function, the *balred* function will attempt to produce a transfer function that yields similar results with less states. This is accomplished by removing states with the smallest Hankel singular values, then modifying the existing states to preserve the original DC gain [13].

To use Matlab's *balred* function, we must identify the transfer function of our compensator. To do so, we first create a state space representation of the compensator spanning the input located at the plant's output and the compensator's output which is fed back into the plant's input. The state space matrix quadruple was found to be:

$$A_{comp} = \begin{bmatrix} A - B_d k - LC & -B_d k_i \\ 0 & 0 \end{bmatrix}$$

$$B_{comp} = \begin{bmatrix} L & -1 \end{bmatrix}^T$$

$$C_{comp} = \begin{bmatrix} k & k_i \end{bmatrix}$$

$$D_{comp} = 0$$

We can use Matlab's *tf* function to generate the transfer function of the compensator. We use the chosen value of $q = 10^6$ in the following.

Figure 9 displays the Bode plot of the original transfer function against the Bode plots of the reduced order transfer functions. It can be seen that the ability to reduce the transfer function states breaks down at the second order. This point is further reinforced when we look at the stability margins for the reduced order models. Table II shows that the phase

margin significantly decreases for a transfer function of the second order, going from 70° for the third order compensator to only 17° for the second order compensator.

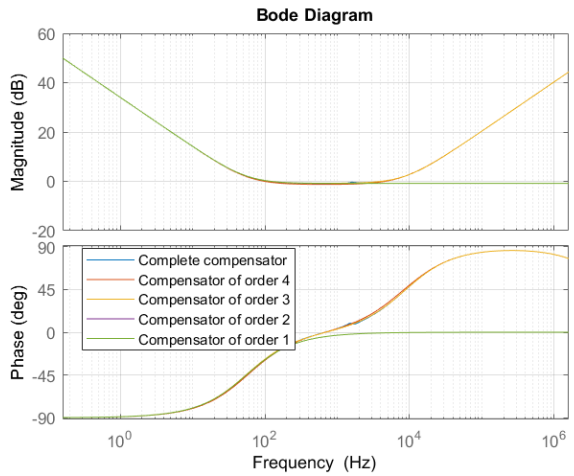

Fig. 9. Model Reduction of compensator

States	Phase Margin	Bandwidth
Unreduced	70	14309
4	71	14378
3	70	14312
2	17	10490
1	17	10490

TABLE II
STABILITY MARGINS FOR MODEL REDUCED LTR COMPENSATOR.

The transfer function, $G_{FOE}(s)$, of the chosen third order compensator is as follows:

$$G_{FOE}(s) = \frac{136 \cdot \left(1 + \frac{s}{5.503 \cdot 10^4}\right)\left(1 + \frac{s}{347}\right)}{s\left(1 + 2.1063 \cdot 10^{-8}s + \left(\frac{s}{6.7142 \cdot 10^7}\right)^2\right)}$$

For validation, we constructed a Simulink model to run the reduced order transfer function. The implementation is shown in Figure 10. As before, we used the disturbance input of a unit step. The results for different order reductions are shown in Figure 11. We show results for compensators of orders 3, 4 and the non-reduced compensator of order 5. As expected, compensator transfer functions of orders 2 and 1 did not simulate well and are therefore not included in Figure 11. Of particular interest is the response of the third order compensator, which is seen to be practically identical to the original full order transfer function response.

VI. Loop Transfer Recovery of Compensator with Reduced Order Estimator

In an effort to further try and reduce the order of the compensator we will now pursue a different tack in the subsequent sections.

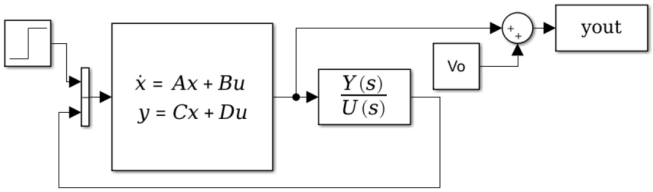

Fig. 10. Simulink system to examine reduced order compensator responses.

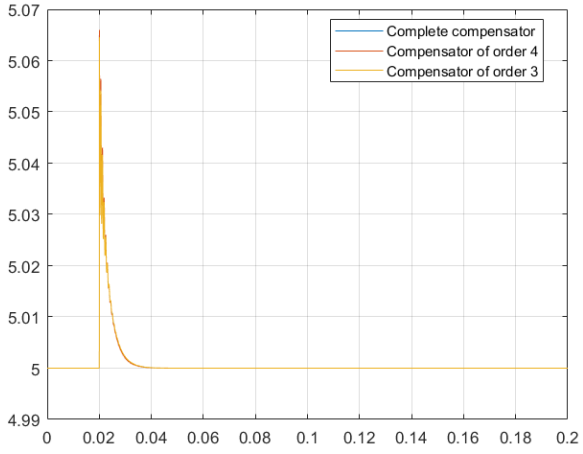

Fig. 11. Model reduction response to unit step input

The previous version of our compensator sought to model each and every state within the plant model. However, in our model the plant output is determined by the vector:

$$C = \begin{bmatrix} 1 & 0 & 0 & 0 \end{bmatrix}$$

Thus for our system, the output of the plant is equivalent to the first state of the plant. In the previous section, we used the full order estimator to estimate the first state (as well as the others). However, since this state variable represents the output, which is already being measured we can use a reduced order estimator to estimate only the remaining three unmeasured states.

For visualization, the compensator with reduced order estimator was modeled in Simulink. The model is shown in Figure 12.

The full order compensator originally used A, B and D gains to reproduce the states. The reduced order estimator uses modified gain blocks which are found with the following relationships:

$$D = A_{22} - LA_{12}$$

$$F = DL + A_{21} - LA_{11}$$

$$G = B_{d2} - LB_{d1}$$

where A and B are partitioned with measured states in the first row and column and unmeasured states in the second and higher rows and columns. Matrices A_{11}, A_{12}, A_{21} and A_{22}

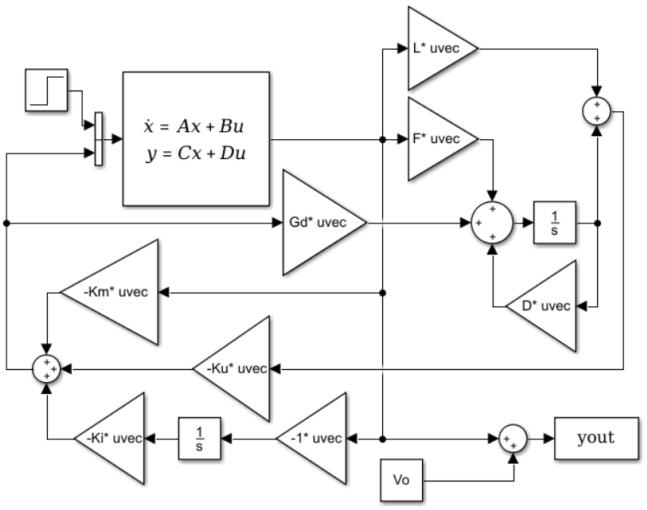

Fig. 12. Simulink diagram of compensator with reduced order estimator.

are the partitioned matrices from matrix A and B_{d1} and B_{d2} are the partitions from vector B_d.

To include the new reduced order estimator in our compensator, we must split the state feedback vector k. Similar to how we divided the coefficients of the state space representation, we split k into k_m and k_u. The gain k_m is applied to states measured directly from the output and the gain k_u is applied to state estimates produced by the reduced order estimator. The gains themselves are not changed.

As previously done, to design L we apply the LTR procedure iterating through different values of parameter q. The following q values were used:

$$q = \begin{bmatrix} 10^{-7} & 10^{-6} & 10^{-5} \end{bmatrix}$$

More specifically, to find the L value for our reduced order compensator, we followed the technique developed by Madiwale and Williams [12]. Consider a minimum phase system with process noise ω with no measurement noise:

$$\dot{x} = Ax + Bu + W\omega$$

$$y = x_m$$

Because process noise characteristics are unknown, we manipulate W and the corresponding noise spectral density V. We partition them as we partitioned A and B in our design of the reduced order estimator. In a similar fashion to how matrices Q and R were manipulated in the previous LTR section, we modify V with respect to q by the following pattern:

$$V_{11} = W_1 V_1 W_1' + q^2 B_{d1} V_2 B_{d1}'$$

$$V_{12} = W_1 V_1 W_2' + q^2 B_{d1} V_2 B_{d2}'$$

$$V_{22} = W_2 V_1 W_2' + q^2 B_{d2} V_2 B_{d2}'$$

Then with:

$$\bar{A} = A_2 2 - V_{12}' V_{11}^{-1} A_{12}$$

$$\bar{V} = V_2 2 - V_{12}' V_{11}^{-1} V_{12}$$

where V_{11} is nonsingular, the following ARE is solved for Q:

$$\bar{A}Q + Q\bar{A}' - QA_{12}' V_{11}^{-1} A_{12} Q + \bar{V}$$

The filter gain L is then determined from Q by the relationship:

$$L = (QA_{12}' + V_{12}')V_{11}^{-1}$$

We used the following values for V_1, V_2, W_1 and W_2:

$$W_1 = \begin{bmatrix} 10^{-4} & 0 & 0 \end{bmatrix}$$

$$W_2 = \begin{bmatrix} 10^{-5} & 0 & 0 \\ 0 & 10^{-5} & 0 \\ 0 & 0 & 10^{-5} \end{bmatrix}$$

$$V_1 = \begin{bmatrix} 10^{-4} & 0 & 0 \\ 0 & 10^{-4} & 0 \\ 0 & 0 & 10^{-4} \end{bmatrix}$$

$$V_2 = 10^{-5}$$

Using the values of q stated above, we obtain Bode plots for the different loop gains. These are shown in Figure 13. It can be seen that we are able to recover much of the loop transfer function of the LQR compensator. If we compare it to Figure 5 it can be seen that the transfer function even tracks the target feedback loop further into the high frequencies than the FOE/LTR compensator. However, this is not inherently desirable as a greater rate of rolloff at higher frequencies improves noise performance.

As seen in Table III, for the three different values of q we were able to obtain approximately the same values of phase margin and unity gain bandwidth, thus the choice of q is arbitrary for this range of values.

For our design we choose $q = 10^{-6}$, which produces the following L value:

$$L = \begin{bmatrix} -3162.1 & -465.0 & 958.3 \end{bmatrix}^T$$

q	Phase Margin	Bandwidth
Full State Feedback	70	14320
1.00E-07	68	13946
1.00E-06	70	14285
1.00E-05	70	14321

TABLE III
STABILITY MARGINS FOR LTR WITH ROE.

To examine the performance of the ROE/LTR compensator, we implemented the Simulink model of Figure 12 to simulate the closed loop system. As before, we used a unit step disturbance input to the system. The results can be seen in Figure 14. Once again, we see that the results are entirely adequate as the reduced order response deviates little from that of the full order.

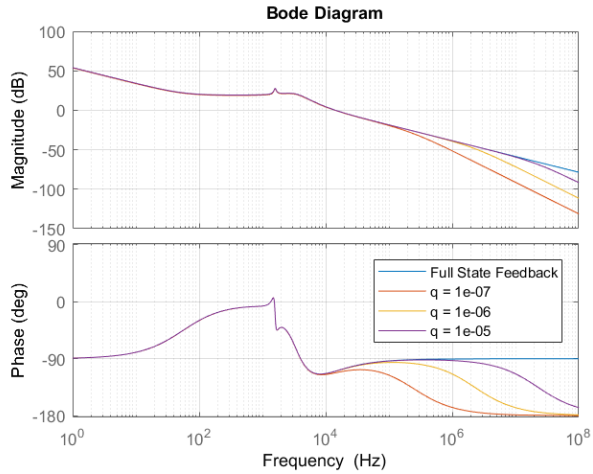

Fig. 13. Bode diagram of open loop system with reduced order estimator undergoing LTR.

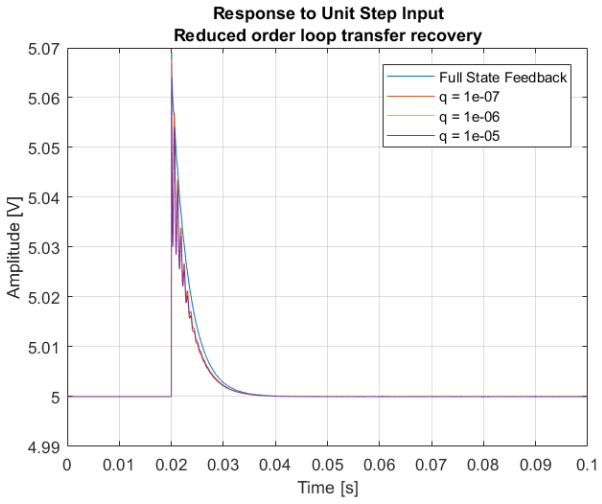

Fig. 14. Simulink results of response to unit step input for the ROE/LTR system.

VII. Model Reduction of Compensator with Reduced Order Estimator.

Now that we have reduced the states in the original compensator by replacing the full order estimator with a reduced order estimator, we pursue even further possible reduction. In the following we used $q = 10^{-5}$, and therefore used its transfer function as our starting point for model reduction.

The compensator with FOE is dominated by a conjugate pair of poles. However the compensator with ROE is dominated by a single real pole. Since the system is dominated by a single pole rather than a pair, we suspect that it is possible to reduce the ROE/LTR compensator more so than we were able with the FOE/LTR compensator.

We once again used Matlab's *balred* function to achieve order reduction. As before, we start by deriving the transfer function of the compensator. To do so we again find a state

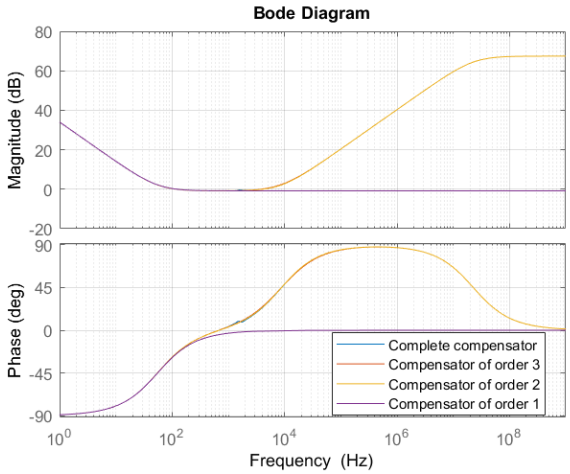

Fig. 15. Model reduction of the ROE/LTR compensator.

Order	Phase Margin	Bandwidth
Unreduced	70	14321
3	70	14520
2	71	14312
1	17	10496

TABLE IV
Stability margins for model reduction of the ROE/LTR compensator.

space representation of the compensator. The state space matrix quadruple is given by:

$$A_{comp} = \begin{bmatrix} D - Gk_u & -Gk_i \\ 0 & 0 \end{bmatrix}$$

$$B_{comp} = \begin{bmatrix} F - Gk_uL - Gk_m & -1 \end{bmatrix}^T$$

$$C_{comp} = \begin{bmatrix} k_u & k_i \end{bmatrix}$$

$$D_{comp} = k_uL + k_m$$

This state space representation is converted to a transfer function using Matlab's *tf* function. The resulting transfer function is used in *balred*.

As can be seen in Figure 15, the transfer function reductions of orders 2 and 3, closely match the original transfer function. Order reduction to one is seen as unacceptable. This observation is confirmed by the phase margin and unity gain bandwidth results shown in Table IV. The phase margin is an optimum 70° until the compensator is reduced to a single state. The transfer function, $G_{ROE}(s)$, of our final, second order compensator is as follows:

$$G_{ROE}(s) = \frac{316 \cdot \left(\frac{s}{54825} + 1\right)\left(\frac{s}{349} + 1\right)}{s\left(\frac{s}{1.424 \cdot 10^8} + 1\right)}$$

In order to double check the performance of our compensator with reduced order estimator, we reused the Simulink model shown in Figure 10. Once again, the input was a unit step. The output response results are shown in Figure 16. It

is of interest that even when we reduce the compensator to first order, the response still takes the desired shape however with a higher overshoot. Nevertheless, as mentioned above, the first order compensator is unsatisfactory given its reduced phase margin shown in Table IV.

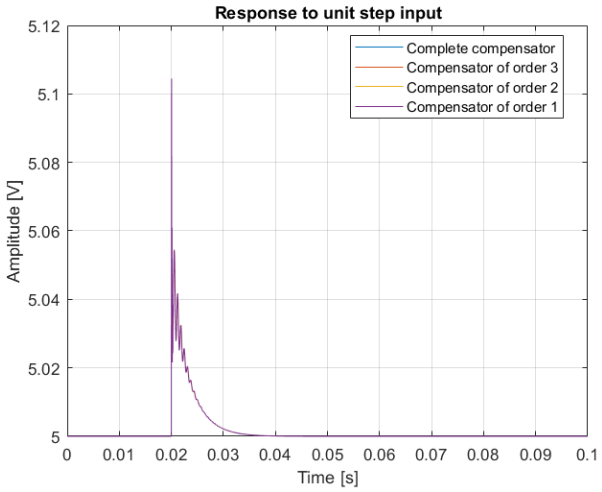

Fig. 16. Simulink response to model reduction of the ROE/LTR compensator.

VIII. Implementation in Circuit Simulation

By reducing the order of the estimator, we were able to produce a transfer function for our compensator that is second order which can be implemented practically with a single op-amp circuit as shown in Figure 17.

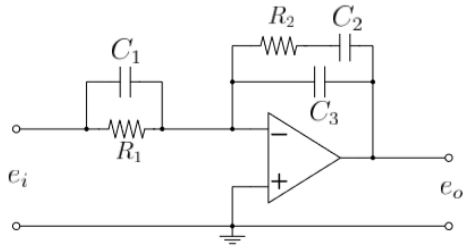

Fig. 17. Second order compensator practical implementation.

The transfer function is given by:

$$G_c(s) = -\frac{\omega_o}{s}\frac{(1+s/\omega_{z1})(1+s/\omega_{z2})}{(1+s/\omega_p)}$$

With a known value for C_3, we may derive values for the other components of the compensator:

$$R_2 = \frac{1}{\omega_p C_3}$$

$$C_2 = \frac{1}{\omega_{z1} R_2}$$

$$R_1 = \frac{1}{\omega_o C_2}$$

$$C_1 = \frac{1}{\omega_{z2} R_1}$$

Arbitrarily setting C_3 to 10 pF, we arrive at the following preferred values:

$$R_2 = 680\ \Omega$$

$$C_2 = 27\ \text{nF}$$

$$R_1 = 120\ \text{k}\Omega$$

$$C_1 = 22\ \text{nF}$$

The compensated system is shown, as a PECS schematic, in Figure 18. Note that, apart from the C1 converter and the just designed second order filter, a pulse width modulator element, output voltage divider (using two 100 Ω resistors) and a voltage reference (using a 2.5 V dc source) has been added to complete the system.

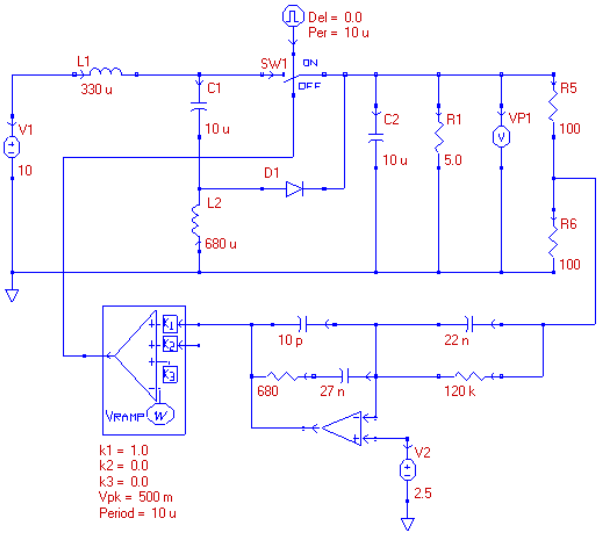

Fig. 18. The C1 converter PECS schematic featuring the final compensator design.

Using the PECS simulator, we examined the disturbance rejection of the closed loop system. An input disturbance is achieved by stepping the input voltage from 10 V to 11 V back to 10 V. The resulting output is shown in Figure 19. As expected, the output waveform mimics that obtained from prior Simulink simulations. Note that there is some slight ringing in the waveform, that was also present in the Simulink obtained responses. As noted previously, for simplicity in our prior modelling, the input disturbance was not made available to the estimator. This results in the slight ringing appearing. If desired, one is able to dampen this oscillation by placing a series connection of an 82 μF capacitor and 8.2 Ω resistor, across capacitor C_1. The response with these damping components added is shown in Figure 20.

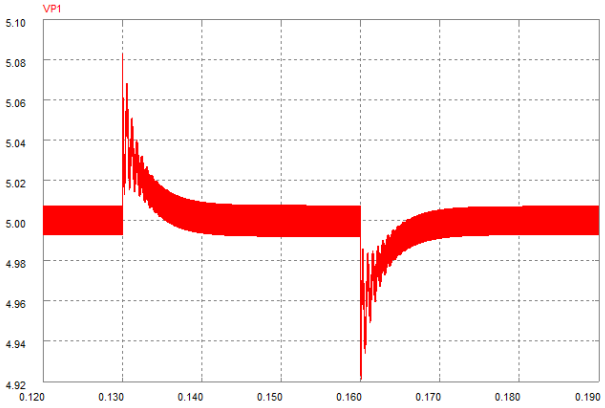

Fig. 19. Output of the C1 converter featuring the final second order compensator design obtained from the PECS simulation. The input disturbance is achieved by stepping the input voltage from 10 V to 11 V back to 10 V.

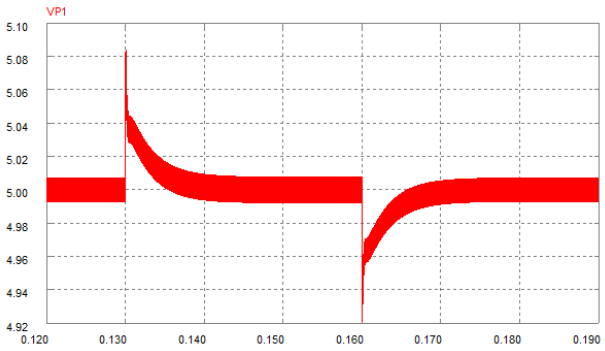

Fig. 20. Output of the C1 converter with damping components added. As before, the input disturbance is achieved by stepping the input voltage from 10 V to 11 V back to 10 V.

IX. Conclusions

Two related compensator design procedures in the modern control theory domain have been undertaken. The system to be controlled was a fourth order dc-to-dc switching power converter. In the first common part of each procedure, a vector of feedback gains was derived by which full state feedback can be effected. A linear quadratic regulator (LQR) design approach was used. In the next step, a full order estimator with added integral feedback was designed using a loop transfer transfer (LTR) procedure to maintain good loop gain properties. The controller gains together with estimator and integral control comprise a compensator. The transfer function of this compensator was next order reduced to a level where good performance was still maintained. Order reduction is undertaken by eliminating states whose corresponding Hankel singular values were relatively small. The whole procedure resulted in the initial fifth order compensator being reduced to one of order three.

The alternative compensator design procedure, starts with the LQR design, which is the same design as before. Since the output of the system which represents one of the system states is a measured quantity, in the next step a reduced order estimator, which estimates the remaining states only, is designed using an appropriate LTR procedure for reduced order estimators. The transfer function of the compensator obtained using the LQR gains and reduced order estimator with integral control has order four. This transfer function was next order reduced which resulted in a second order compensator. This compensator was subsequently implemented in a circuit simulator which confirmed good input disturbance rejection performance of the closed loop system.

This paper has demonstrated that to obtain a minimal order compensator it is best to start with a reduced order estimator followed by order reduction. This compensator subsequently reduces implementation demands without an accompanying loss of performance.

References

[1] W. S. Levine, Ed., "The Control Handbook", Boca Raton FL: CRC Press LLC, 1996.

[2] R. Tymerski and V. Vorperian, "Generation, Classification and Analysis of Switched-Mode DC-to-DC Converters by the Use of Converter Cells," INTELEC '86 - International Telecommunications Energy Conference, Toronto, Canada, 1986, pp. 181-195, doi: 10.1109/INTLEC.1986.4794425.

[3] R. Tymerski, V. Vorperian, "Generation and classification of PWM DC-to-DC converters", Aerospace and Electronic Systems IEEE Transactions on, vol. 24, no. 6, pp. 743-754, 1988.

[4] M. Veerachary, "Two-loop voltage-mode control of coupled inductor step-down buck converter", IEE Proceedings - Electric Power Applications, vol. 152, pp. 1516, 2005.

[5] M. Veerachary, "Analysis of Minimum-Phase Fourth-Order Buck DC–DC Converter," in IEEE Transactions on Industrial Electronics, vol. 63, no. 1, pp. 144-154, Jan. 2016, doi: 10.1109/TIE.2015.2472525.

[6] D. Li, R. Tymerski and T. Ninomiya, "PECS. An efficacious solution for simulating switched networks with nonlinear elements," 2000 IEEE 31st Annual Power Electronics Specialists Conference. Conference Proceedings (Cat. No.00CH37018), Galway, Ireland, 2000, pp. 274-279 vol.1, doi: 10.1109/PESC.2000.878856.

[7] D. Li, R. Tymerski and T. Ninomiya, "PECS-an efficient solution for simulating switched networks with nonlinear elements," in IEEE Transactions on Industrial Electronics, vol. 48, no. 2, pp. 367-376, April 2001, doi: 10.1109/41.915415.

[8] R. D. Middlebrook and S. Cuk, "A general unified approach to modelling switching-converter power stages," 1976 IEEE Power Electronics Specialists Conference, Cleveland, OH, 1976, pp. 18-34, doi: 10.1109/PESC.1976.7072895.

[9] G. C.Verghese, "Dynamic modelling and control in power electronics," in The Control Handbook, W. S. Levine, Ed. Boca Raton FL: CRC Press LLC, 1996, ch. 78.1, pp. 1413-1424.

[10] J. Doyle, "Guaranteed margins for LQG regulators," in IEEE Transactions on Automatic Control, vol. 23, no. 4, pp. 756-757, August 1978, doi: 10.1109/TAC.1978.1101812.

[11] J. Doyle and G. Stein, "Robustness with observers," in IEEE Transactions on Automatic Control, vol. 24, no. 4, pp. 607-611, August 1979, doi: 10.1109/TAC.1979.1102095.

[12] A. N. Madiwale and D. E. Williams, "Some Extensions of Loop Transfer Recovery," 1985 American Control Conference, Boston, MA, USA, 1985, pp. 790-795, doi: 10.23919/ACC.1985.4788723.

[13] balred (2020)[online].
Available: https://www.mathworks.com/help/control/ref/balred.html